

# Preparation and Morphology of Sarcoplasmic Reticulum Terminal Cisternae from Rabbit Skeletal Muscle

AKITSUGU SAITO, STEVEN SEILER, ALICE CHU, and SIDNEY FLEISCHER

*Department of Molecular Biology, Vanderbilt University, Nashville, Tennessee 37235. Dr. Seiler's present address is Department of Pharmacology, Indiana University School of Medicine, Krannert Institute of Cardiology, Indianapolis, Indiana 46202.*

**ABSTRACT** We have developed a procedure to isolate, from skeletal muscle, enriched terminal cisternae of sarcoplasmic reticulum (SR), which retain morphologically intact junctional "feet" structures similar to those observed in situ. The fraction is largely devoid of transverse tubule, plasma membrane, mitochondria, triads (transverse tubules junctionally associated with terminal cisternae), and longitudinal cisternae, as shown by thin-section electron microscopy of representative samples. The terminal cisternae vesicles have distinctive morphological characteristics that differ from the isolated longitudinal cisternae (light SR) obtained from the same gradient. The terminal cisternae consist of two distinct types of membranes, i.e., the junctional face membrane and the  $\text{Ca}^{2+}$  pump protein-containing membrane, whereas the longitudinal cisternae contain only the  $\text{Ca}^{2+}$  pump protein-containing membrane. The junctional face membrane of the terminal cisternae contains feet structures that extend  $\sim 12$  nm from the membrane surface and can be clearly visualized in thin section through using tannic acid enhancement, by negative staining and by freeze-fracture electron microscopy. Sections of the terminal cisternae, cut tangential to and intersecting the plane of the junctional face, reveal a checkerboardlike lattice of alternating, square-shaped feet structures and spaces each 20 nm square. Structures characteristic of the  $\text{Ca}^{2+}$  pump protein are not observed between the feet at the junctional face membrane, either in thin section or by negative staining, even though the  $\text{Ca}^{2+}$  pump protein is observed in the nonjunctional membrane on the remainder of the same vesicle. Likewise, freeze-fracture replicas reveal regions of the P face containing ropelike strands instead of the high density of the 7–8-nm particles referable to the  $\text{Ca}^{2+}$  pump protein. The intravesicular content of the terminal cisternae, mostly  $\text{Ca}^{2+}$ -binding protein (calsequestrin), is organized in the form of strands, sometimes appearing paracrystalline, and attached to the inner face of the membrane in the vicinity of the junctional feet. The terminal cisternae preparation is distinct from previously described heavy SR fractions in that it contains the highest percentage of junctional face membrane with morphologically well-preserved junctional feet structures.

The muscle fiber contains an intricate membraneous network that controls muscle contraction and relaxation by regulating the intracellular calcium concentration. The plasma membrane or plasmalemma invaginates transversely into the muscle sarcoplasm to form transverse tubules, which are connected to an internal reticular membrane system, the sarcoplasmic reticulum (SR).<sup>1</sup> The SR surrounds the sarcomere in

a sleeve-like manner, and is composed of two distinct portions: (a) the terminal cisternae which are junctionally associated with the transverse tubule, and (b) the longitudinal cisternae or longitudinal SR, which connect medially with the two terminal cisternae. The terminal cisternae are connected to the transverse tubule via junctional structures referred to as "feet" (6, 13, 14, 20, 31, 36). The major component of the SR membrane is the  $\text{Ca}^{2+}$  pump protein, which has a molecular weight of  $\sim 115,000$ . This protein is responsible for the

<sup>1</sup> *Abbreviation used in this paper:* SR, sarcoplasmic reticulum.

characteristic asymmetric appearance of the membrane (34).

The present study describes the isolation and morphological characterization of enriched terminal cisternae and compares them with light SR referable to longitudinal cisternae.

## MATERIALS AND METHODS

**Electron Microscopy:** Fixation of samples in 2% glutaraldehyde with or without 1% tannic acid for thin-section electron microscopy was performed as described previously (33, 34). Representative sampling of thin sections was ensured by using the filter procedure described by Palade et al. (30) or by using small pellets and examining complete sections cut perpendicular to the axis of centrifugation. The percentage of surface area of the terminal cisternae occupied by the "feet" structure and thereby referable to junctional face membrane was measured using a Dietzen (Chicago, IL) map measure on electron micrographs of thin sections. The ratio of the length of the junctional face occupied by the feet to that of the total membrane perimeter of all the vesicles was determined. The prints were enlarged  $\times 200,000$ ; the original negative was  $\times 50,000$ . The standard deviation of the distance measurement was 3%. The values presented were obtained with 500 representative cross sections of vesicles. For negative staining or freeze-fracture the samples were fixed, in suspension, for at least 2 h at  $0-4^{\circ}\text{C}$  in 2% (vol/vol) glutaraldehyde, 8% (wt/vol) sucrose, 10 mM sodium cacodylate, pH 7.2. The samples for negative staining were then treated with 1% (wt/vol) phosphotungstic acid, adjusted to pH 7.2 with NaOH and prepared for examination (8, 33). For freeze-fracture, the glutaraldehyde-fixed samples were sedimented and then infiltrated with 30% glycerol. Freeze-fracture and preparation of replicas, including rotary shadowing, was as previously described (33, 34). As before, shadowing was initiated within 2 s after fracture.

**Biochemical Assay:**  $[\text{Ca}^{2+}, \text{Mg}^{2+}]\text{ATPase}$  activity was measured at  $25^{\circ}\text{C}$  in the presence of  $1.5 \mu\text{g}$  of A23187/ml,  $100 \mu\text{M}$   $\text{CaCl}_2$ ,  $60 \mu\text{M}$  potassium EGTA,  $100 \text{ mM}$  KCl,  $5 \text{ mM}$   $\text{MgCl}_2$ ,  $0.3 \text{ M}$  sucrose,  $5 \text{ mM}$   $\text{Na}_2\text{ATP}$ ,  $5 \text{ mM}$  potassium HEPES, pH 7.0, and  $10 \mu\text{g}$  of protein/ml using a coupled-enzyme assay containing  $8.5 \text{ U/ml}$  of pyruvate kinase,  $12 \text{ U/ml}$  of lactic dehydrogenase,  $400 \mu\text{M}$  NADH, and  $2 \text{ mM}$  phosphoenolpyruvate (39). The  $[\text{Ca}^{2+}, \text{Mg}^{2+}]\text{ATPase}$  activity was the difference between the linear rates measured in the presence of  $\text{Ca}^{2+}$  and that in its absence (with  $4 \text{ mM}$  potassium EGTA).

Phospholipid phosphorus was quantitated as described by Rouser and Fleischer (32), and protein was measured according to the method of Lowry et al. (24) using bovine serum albumin as a standard. Slab PAGE in the presence of sodium dodecyl sulfate was carried out according to Laemmli (21), with 3% stacking gel and 8% resolving gel. The gels were stained with Coomassie Brilliant Blue R-250. Protein standards used were, in molecular weight, phosphorylase b (92,500), bovine serum albumin (66,200), and ovalbumin (45,000).

**Isolation of SR Terminal and Longitudinal Cisternae:** New Zealand white female rabbits (1–3 kg weight) were killed by cervical dislocation, and all subsequent steps were carried out at  $0-4^{\circ}\text{C}$ . The predominantly white portions of the hind leg muscles<sup>2</sup> were separated away from muscle which was pink in appearance and connective tissue. Dissection was performed on a glass tray seated on packed ice. The muscle was ground in a meat grinder (General Model H meat grinder) with a faceplate having 2-mm holes. The ground meat, in 50 g portions, was homogenized in 250 ml of 0.3 M sucrose, 5 mM imidazole-HCl, pH 7.4 (homogenization medium), using a Waring blender (Waring Products Div., New Hartford, CT) at maximum speed for one min. The homogenate was centrifuged in a JA 10 rotor (Beckman Instruments, Inc., Fullerton, CA; model J-21 centrifuge) for 10 min at 8,000 rpm ( $7,700 g_{\text{max}}$ ). The supernatant (S1) was saved during initial studies, and the pellets were rehomogenized as before in another 250 ml of homogenization medium. The rehomogenate was kept ice-cold and again centrifuged as before and the supernatant (S2) saved. The longitudinal and terminal cisternae of SR were obtained from the S2 supernatant. The supernatant was filtered through 3–4 layers of cheesecloth, and a microsomal pellet was obtained by centrifugation for 90 min at 30,000 rpm ( $110,000 g_{\text{max}}$ ) in a Beckman 35 rotor. The microsomes were resuspended in homogenization medium (11 ml) using a Dounce homogenizer and layered onto a sucrose step gradient, one 250-ml homogenate equivalent per one to two gradient tubes. The gradient steps, 7 ml each, consisted of 45% (wt/wt) sucrose (1.6 M), 38% sucrose (1.3 M), 32% sucrose (1.1 M), and 27% sucrose (0.8 M), all buffered with 5 mM imidazole-HCl, pH 7.4. The gradients were centrifuged overnight (14–16 h) in a Beckman SW 27 rotor at 20,000 rpm ( $70,000 g_{\text{max}}$ ). The membrane fractions at the interfaces between the gradient steps (Fig. 1) were collected, diluted approximately twofold with 5 mM imidazole-HCl, pH 7.4, and centrifuged in a Beckman 35 rotor for

<sup>2</sup> The predominantly white muscles or portions thereof were sartorius, gracilis, vastus lateralis, vastus medialis, adductor magnus, gluteus (maxima, medius, minimus), biceps femoris, and gastrocnemius.

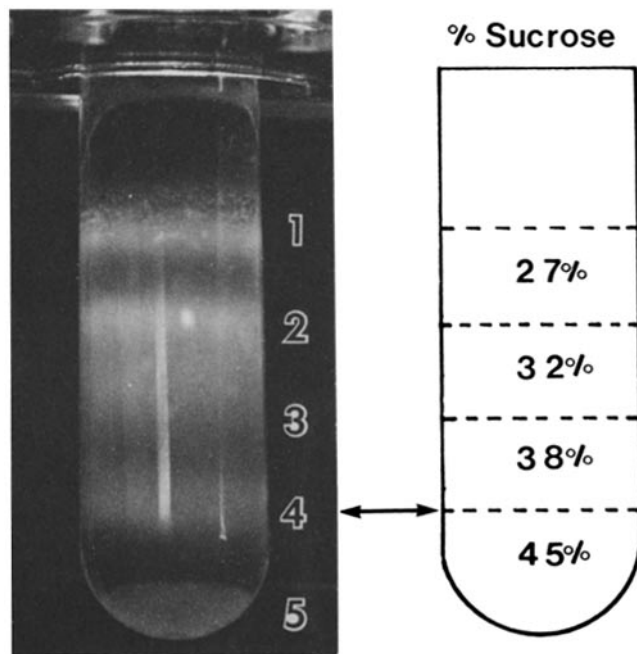


FIGURE 1 Discontinuous sucrose gradient for subfractionation of muscle microsomes (see Materials and Methods). The microsomes obtained from the second homogenization of muscle (S2, cf. Materials and Methods) give rise to a well-defined terminal cisternae fraction ( $R_4$ , arrow). Fraction  $R_2$  is enriched in longitudinal cisternae.

2 h at 32,000 rpm ( $125,000 g_{\text{max}}$ ). The pellets were then resuspended in homogenization medium and quick-frozen in liquid nitrogen, and stored at  $-70^{\circ}\text{C}$  until use.

**Isolation of Light and Heavy SR:** The isolation procedure was essentially as described by Meissner (25), which included 0.6 M KCl in the first zonal centrifugation throughout the layers of the gradient and a final salt extraction of the light and heavy SR fractions.

## RESULTS

### Isolation of Fractions Enriched in SR Terminal and Longitudinal Cisternae

A procedure has been developed for the isolation of terminal and longitudinal cisternae of SR from the same gradient (cf. Materials and Methods). The microsomes obtained from the second rehomogenization of the muscle were subfractionated on a sucrose step gradient centrifuged to equilibrium (Fig. 1). The composition of the different fractions was examined by electron microscopy. Fraction 1 contained mostly SR longitudinal cisternae (or light SR) with some transverse tubules and plasma membrane. Fraction 2, at the 27/32% sucrose interface, was enriched with longitudinal cisternae of SR, although it contained some terminal cisternae as well. Fraction 3 (32/38% interface) contained a mixture of longitudinal and terminal cisternae. Fraction 4 (38/45% interface) consisted of highly enriched terminal cisternae of SR. Fraction 5 contained aggregated contractile protein and intact mitochondria.

The composition of the fractions from the step gradient differed depending on whether the microsomes were obtained from the first or second homogenization of ground muscle. Fraction 4 obtained from microsomes prepared from the first homogenization consisted of vesicles containing electron-opaque contents. Some of these vesicles contained junctional "feet" structures but others did not and resembled more the

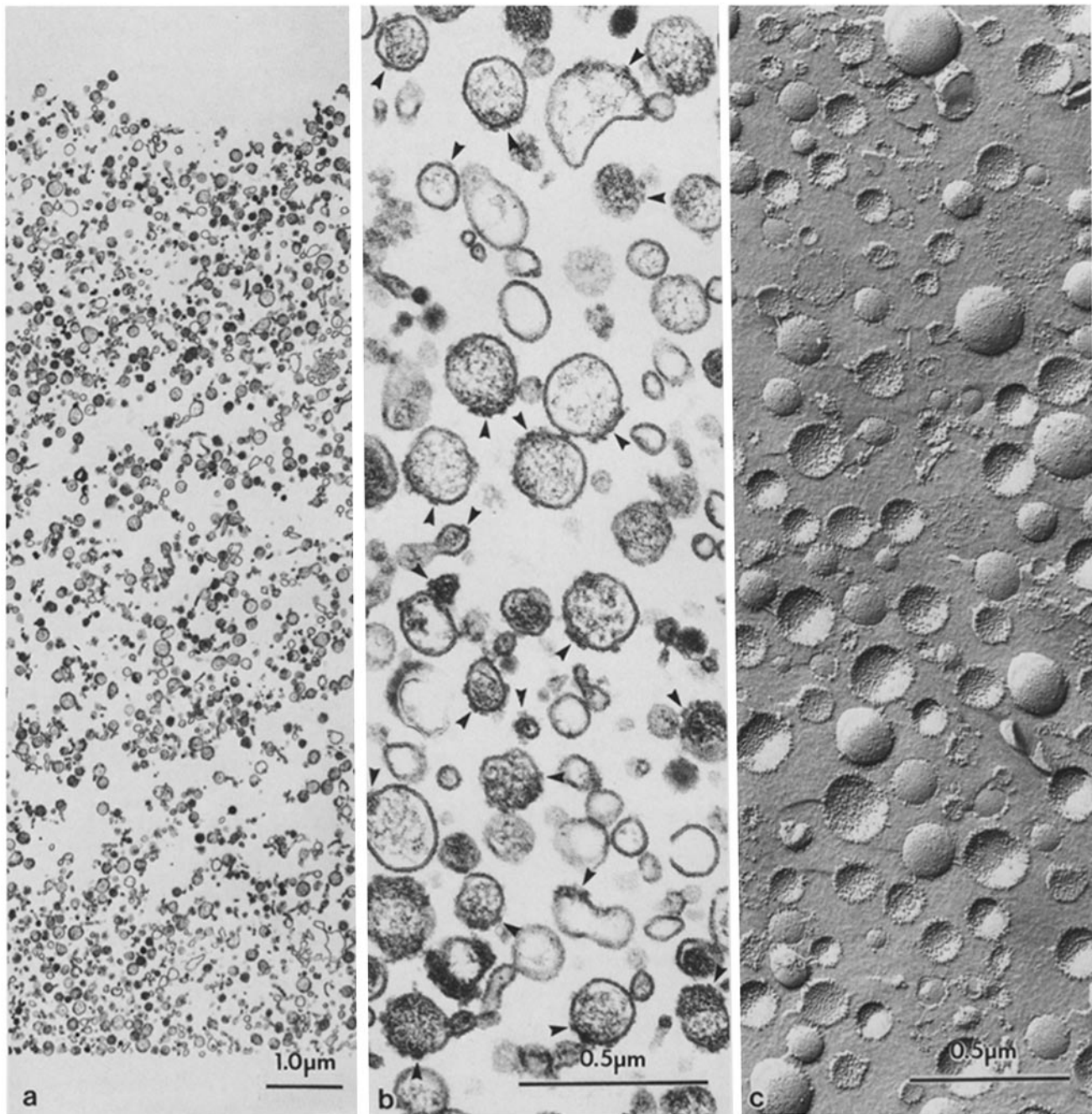


FIGURE 2 Thin-section electron microscopy of the highly enriched terminal cisternae fraction. A sample of fraction  $R_4$ , 50–100  $\mu\text{g}$  of protein, was fixed with tannic acid/glutaraldehyde in 2 ml of dilute suspension and then centrifuged to obtain a thin pellet. The oriented pellet was sectioned perpendicularly to the axis of centrifugation to provide a full cross section.  $\times 12,000$  (a). A higher magnification is shown in thin section ( $\times 60,000$ ) (b) and by freeze-fracture ( $\times 50,000$ ) (c). The fraction consists mainly of spherulike vesicles of sarcoplasmic reticulum terminal cisternae, containing electron-opaque contents (b). Characteristic junctional feet (compare with in situ, Fig. 4f), indicative of the junctional face, can be observed in many of the vesicles (arrowheads). The terminal cisternae vesicles observed in thin section (b) or by freeze-fracture (c) range in size from 70 to 300 nm in diameter.

heavy SR fraction described by Meissner (25) which has not been salt-extracted (not shown). Fraction  $R_4$ , obtained from the second homogenization, consisted of vesicles containing both electron-dense intravesicular contents as well as appreciable numbers of junctional feet structures (Fig. 2). These vesicles thus resemble the terminal cisternae in situ and have been designated “terminal cisternae” vesicles. The terminal cisternae (fraction  $R_4$ ) and longitudinal cisternae (fraction  $R_2$ ) have been characterized in this paper and compared with light and heavy SR (25).

### Biochemical Characterization

The terminal cisternae (fraction  $R_4$ ) are distinctly different from the longitudinal cisternae (fraction  $R_2$ ), in that they have (a) lower lipid-to-protein ratio, (b) lower specific activity of  $[\text{Ca}^{2+}, \text{Mg}^{2+}] \text{ATPase}$ , and (c) high content of  $\text{Ca}^{2+}$ -binding protein (calsequestrin). These differences can be explained by the high content of  $\text{Ca}^{2+}$ -binding protein in the terminal cisternae, approximating half that of the  $\text{Ca}^{2+}$  pump protein on a weight basis (Table I, Fig. 3). Morphological studies,

TABLE I  
Biochemical Characterization of Membrane Fractions from  
Skeletal Muscle

	Yield*	Phospholipid content	Ratio* of CBP/ CPP	[Ca <sup>2+</sup> , Mg <sup>2+</sup> ] ATPase + A23187
	mg	μmol P/mg protein		μmol/min per mg protein
Microsomes	66	0.84	—	—
Fraction R <sub>1</sub>	2	1.13	0.10	2.3
Fraction R <sub>2</sub>	12	0.65	0.11	3.7
Fraction R <sub>3</sub>	9	0.55	0.30	2.7
Fraction R <sub>4</sub>	6	0.52	0.50	2.5
Light SR	4	0.90	0.056	3.4
Heavy SR	4	0.52	0.46	3.0

Fractions R<sub>1</sub>–R<sub>4</sub> were prepared from microsomes obtained from the second homogenization (cf. Materials and Methods). Light and heavy SR were prepared according to a modification of Meissner, in the presence of 0.6 M KCl (25).

\* From 50 g wet weight of muscle (average results from at least three preparations are presented).

\* Obtained from densitometric tracings of SDS polyacrylamide gels stained with Coomassie Brilliant Blue (as described in Fig. 3). CBP, Ca<sup>2+</sup>-binding protein (calsequestrin); CPP, Ca<sup>2+</sup> pump protein.

described below, show that a portion of the terminal cisternae is junctional face membrane, which is distinct from the more common Ca<sup>2+</sup> pump-containing membrane, contributing in small part (~16%, see below) to the reduced [Ca<sup>2+</sup>, Mg<sup>2+</sup>] ATPase specific activity of fraction R<sub>4</sub>. A high-molecular-weight component was observed in the terminal cisternae fraction which was not found in the longitudinal cisternae (fraction R<sub>2</sub>) and light SR (Fig. 3). Cadwell and Caswell (2) have suggested that high molecular weight proteins are components of the junctional feet. The longitudinal and terminal cisternae fractions are both capable of Ca<sup>2+</sup> transport (Chu, A., P. Volpe, B. Costello, and S. Fleischer, manuscript in preparation). The longitudinal cisternae (fraction R<sub>2</sub>) are contaminated in part by terminal cisternae (~20%) as indicated by thin-section electron microscopy and by the content of Ca<sup>2+</sup> binding protein (Table I). The yield of longitudinal (fraction R<sub>2</sub>) and terminal (fraction R<sub>4</sub>) cisternae is greater than that for the light and heavy SR described by Meissner (25). Additional light and heavy SR is also obtainable from the first supernatant (S1).

### Morphology of Isolated SR Terminal and Longitudinal Cisternae Vesicles

The uniformity of the terminal cisternae fraction was assessed using complete sections cut perpendicular to the axis of centrifugation (Fig. 2*a*). Thin-section and freeze-fracture electron microscopy indicate largely terminal cisternae vesicles ranging between 70 and 300 nm in diameter (Fig. 2, *b* and *c*), as compared with 200 nm for the light SR and 70–100 nm for heavy SR.

Both terminal cisternae vesicles and heavy SR contain electron-dense contents, whereas the longitudinal cisternae and light SR lack such contents (Fig. 4). The unique feature of this terminal cisternae fraction is the relatively high percentage of junctional face membrane containing well-preserved junctional feet structures. We find from thin-section electron microscopy that roughly 38% of the sections of vesicles exhibited these structures. Of the sections which have feet structures, on the average, 34% of the perimeter was

covered with the junctional feet. The percentage of surface area, of all the section measured, occupied by the feet was found to be 16%. The larger vesicles or sections had a higher percentage of junctional face. The remainder of the membrane of the terminal cisternae consists of Ca<sup>2+</sup> pump-containing membrane. The junctional face of the isolated terminal cisternae of SR is morphologically similar to that in situ, where it is junctionally associated with the transverse tubule.

There is considerable variation in the appearance, in thin sections, in the percentage of junctional face at the perimeter of the vesicles (Fig. 4, *a–c*). In the extreme case, junctional feet were observed over the entire perimeter of the section (Fig. 4*c*), suggesting that this portion of the vesicle derived entirely from the junctional face.

The longitudinal cisternae vesicles appear to consist of a single type of membrane composed largely of the Ca<sup>2+</sup> pump protein (Fig. 3). We have designated this membrane "the Ca<sup>2+</sup> pump-containing membrane." The characteristics of this membrane by three different methods of sample preparation for electron microscopy are: (*a*) a highly asymmetric trilayer membrane (7, 2, 2 nm) observed in thin section with tannic

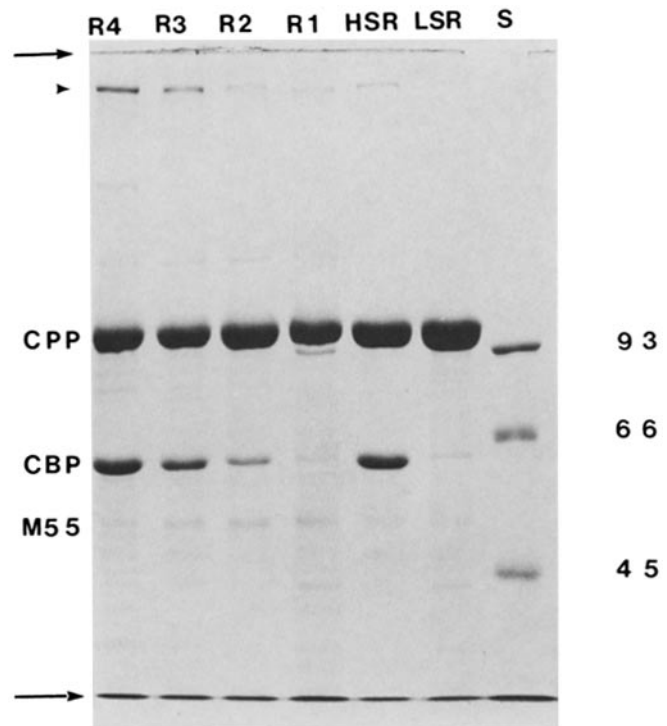


FIGURE 3 SDS PAGE of sucrose gradient fractions. The gradient fractions, R<sub>1</sub>–R<sub>4</sub> (see Fig. 1) were loaded onto the stacking gel (Materials and Methods). The arrows denote the beginning of the resolving gel (top) and the dye front (bottom). Protein standards (S) are shown in the last lane. The molecular weight standards ( $\times 10^{-3}$ ) were phosphorylase b (92.5), bovine serum albumin (66.2), and ovalbumin (45). Fractions of light (LSR) and heavy sarcoplasmic reticulum (HSR), prepared by modification of the method described by Meissner (25), are presented for comparison. 8 μg each of the various fractions of SR were applied. The Ca<sup>2+</sup> pump protein (CPP), Ca<sup>2+</sup>-binding protein (calsequestrin (CBP)), and a 55,000-mol-wt protein (M<sub>55</sub>) are indicated. The terminal cisternae preparation (R<sub>4</sub>) is rich in Ca<sup>2+</sup>-binding protein as compared with longitudinal cisternae (R<sub>2</sub>) and light SR. Note the intense high molecular weight component (arrowhead) as well as smaller molecular weight components in the terminal cisternae fraction which are present to only a small extent in heavy SR and are essentially absent in the light SR.

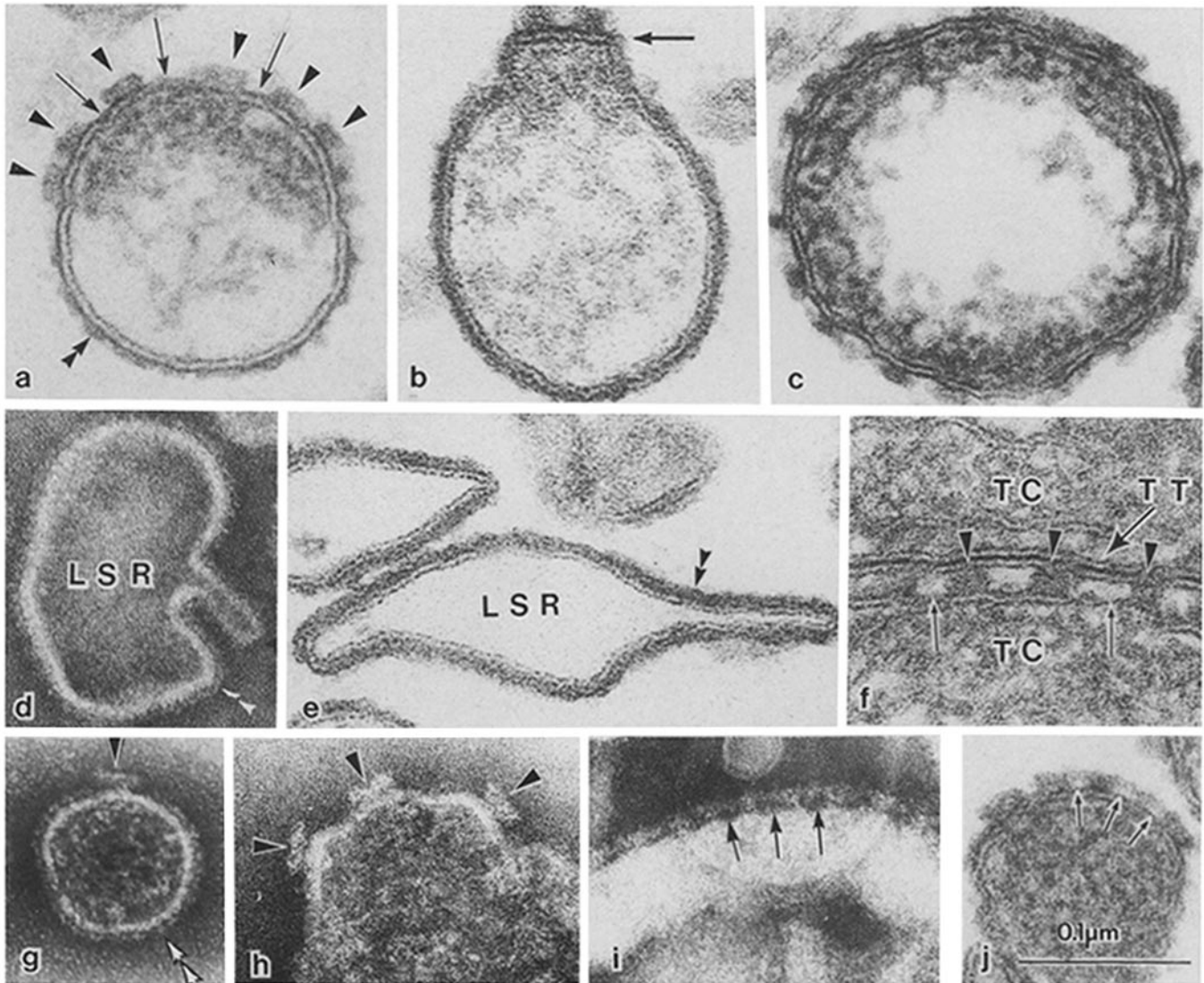


FIGURE 4 Comparison of SR terminal cisternae vesicles with light SR. Terminal cisternae vesicles, observed in thin section (a–c and j) and by negative staining (g, h, and i), consist of two types of membranes. One corresponds to the junctional face containing the feet structures (arrowheads), while the other is the  $\text{Ca}^{2+}$  pump-containing membrane (double arrowheads). The lumen of the terminal cisternae vesicles contain electron-opaque contents which appear to be attached to the junctional face. The junctional face membrane contains feet structures (arrowheads) that project 12 nm from the surface of the membrane with a repeat spacing of 40 nm. Note the absence of surface material characteristic of the  $\text{Ca}^{2+}$  pump protein (arrow) between the junctional feet (arrows, a–c and f, in situ). The terminal cisternae sections vary widely in the percentage of junctional face membrane observed at the perimeter, i.e., only a small portion (b in thin section, and g, negative staining), about half (a) to nearly all (c). Sometimes adjacent feet structures appear continuous with one another (note arrows in i and j). On occasion the junctional face membrane appears flat (b, arrow). The junctional face membrane of the terminal cisternae retains the characteristic morphology observed in situ in thin sections (f). The separation between transverse tubule and terminal cisternae membranes of the triad junction, in situ, is approximately 13 nm (f). TC, terminal cisternae; TT, transverse tubule. Light SR, referable to longitudinal cisternae, consist only of the  $\text{Ca}^{2+}$  pump-containing membrane observed in thin section (e) or by negative staining (d).  $\times 260,000$ .

acid enhancement (34) (Fig. 4e); (b) 3–4-nm particles on the outer face by negative staining (16) (Fig. 4d); and (c) a highly asymmetric distribution of 7–8-nm particles mostly in the P face as observed by freeze fracture (5) (Fig. 6, c and d). These features are referable to the  $\text{Ca}^{2+}$  pump protein (34). The longitudinal cisternae fraction described in this study has essentially the same morphology as the light SR (25).

The junctional face-containing membrane has been characterized by electron microscopy using three methods of sample preparation. It is distinctly different from the  $\text{Ca}^{2+}$  pump-containing membrane (34) (Figs. 4–6). Thin-section

electron microscopy with tannic acid enhancement reveals that the feet structures are ~20 nm in width with a repeat spacing of ~40 nm and extending 12 nm from the surface of the membrane (Fig. 4). The junctional feet can be observed as discrete units separated from one another (Fig. 4, a and c). When viewed in thin section using tannic acid enhancement, the surface between the junctional feet structures is devoid of material characteristic of  $\text{Ca}^{2+}$  pump proteins (Fig. 4, a and c), even though the  $\text{Ca}^{2+}$  pump-containing membrane is observed elsewhere on the same section of the vesicles (Fig. 4, a and b). Stain penetration was clearly not a problem in these



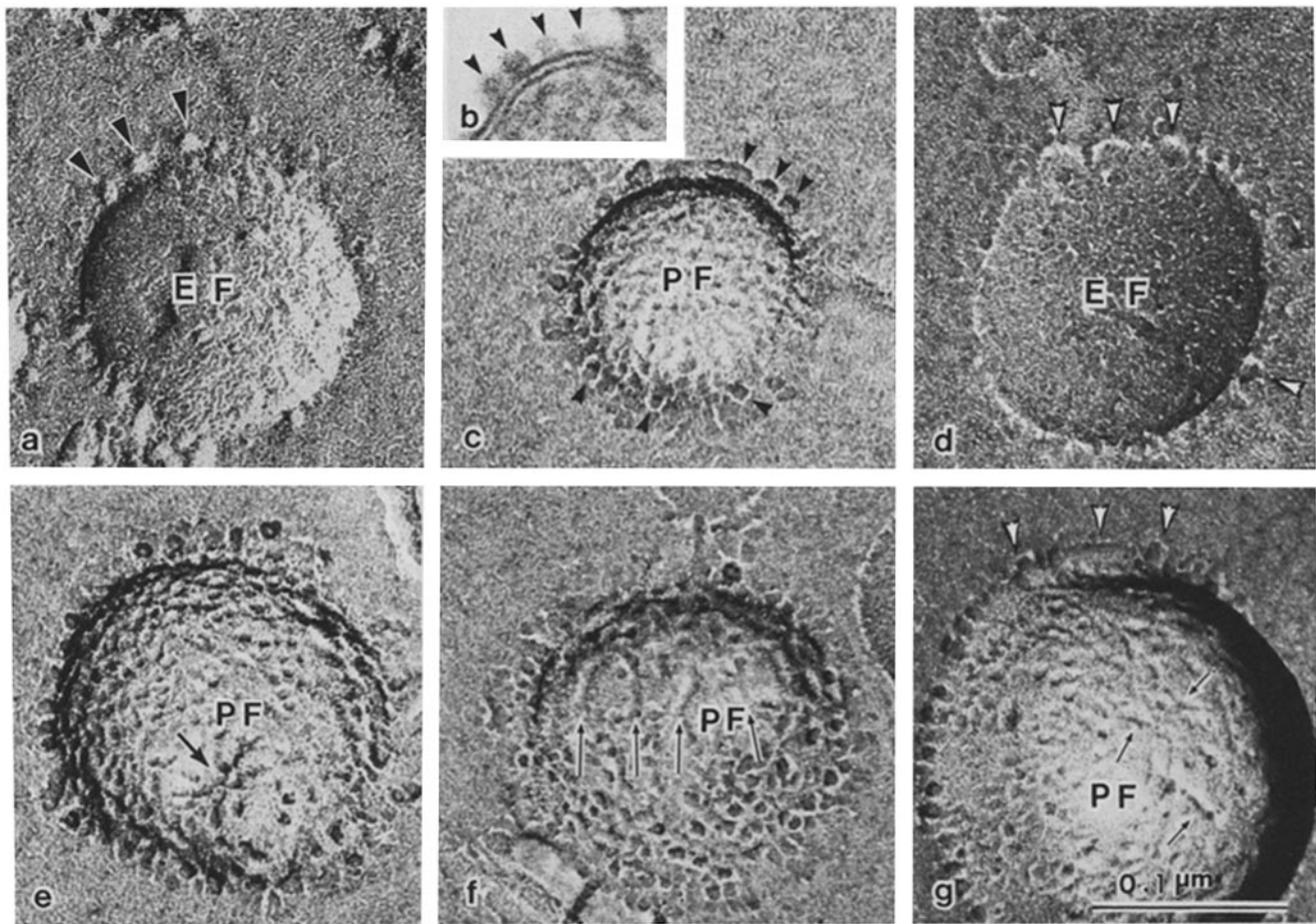


FIGURE 5 Freeze-fracture replicas of terminal cisternae. Junctional feet are denoted by arrowheads and can be observed in both the E and P faces (a, c, and d). In a, conventional shadowing was used; the remainder were rotary shadowed. The spacing and dimensions of the feet structures (arrowheads) are comparable to those observed in thin section (b). The P face has regions of low particle density containing ropelike strands (arrows, e-g) with different arrangements, spokelike (e), approximating parallel arrays (f) and more random (g), which are never seen in light SR and appear to be referable to the junctional face membrane. The ropelike strands are not observed on the E face of the terminal cisternae (d).  $\times 260,000$ .

sections, because the internal contents of the terminal cisternae vesicles were heavily stained. In situ, the triad junction also reveals a junctional face membrane devoid of surface structures characteristic of the  $\text{Ca}^{2+}$  pump protein (Fig. 4f). In contrast with the longitudinal cisternae, which have a uniform broad outer layer (Fig. 4d), some areas of the  $\text{Ca}^{2+}$  pump-containing membrane of terminal cisternae appear patchy in thin-section micrographs after tannic acid enhancement (Fig. 4, a vs. e).

The junctional feet are also clearly observed by negative staining to project from the surface of the junctional face of the terminal cisternae vesicles and are clearly distinguishable from the 3–4-nm particles referable to  $\text{Ca}^{2+}$  pump protein (Fig. 4, h vs. d). The dimensions of the junctional feet structures observed by negative staining are comparable to those observed in thin sections with tannic acid enhancement. The absence of  $\text{Ca}^{2+}$  pump protein between the junctional feet structures was similarly confirmed by negative staining (Fig. 4h) by the absence of 3–4-nm particles at the surface even though such particles were observed elsewhere on the same vesicle (Fig. 4g). By contrast, the entire surface of longitudinal cisternae SR vesicles is uniformly studded with these surface particles (Fig. 4d).

Freeze-fracture (Fig. 5) reveals feet structures of comparable dimensions to those observed in thin section (Fig. 4, a–c) and by negative staining (Fig. 4h). These are seen in both the E (Fig. 5, a and d) and P faces (Fig. 5, c and g). Some regions of the fracture faces of terminal cisternae look distinctly different from the longitudinal cisternae vesicles. In such regions, the P face is devoid of particles or considerably reduced in particle density. Instead, ropelike strands can be observed (Fig. 5, e–g) which are not seen in the E face. Such regions are undoubtedly referable to the junctional face membrane. By contrast, the P face of the longitudinal cisternae vesicles reveals a high density of 8-nm particles, referable to the  $\text{Ca}^{2+}$  pump protein (Fig. 6d).

Freeze-fracture reveals two structures in the terminal cisternae other than the feet in the terminal cisternae which are not observed in the longitudinal cisternae: (a) filaments are observed at the hydrophobic center of the P face (Fig. 5, e–g). Such filaments appear to be the anchoring of the intravesicular paracrystalline or ropelike arrays observed in thin section or negative staining; (b) the E face of some terminal cisternae vesicles reveal 4–5-nm (in diameter) pits separated by  $\sim 30$ – $34$ -nm repeat distances (Fig. 6a). Such pits have been observed in situ (12), but the relationship, if any, of the pits

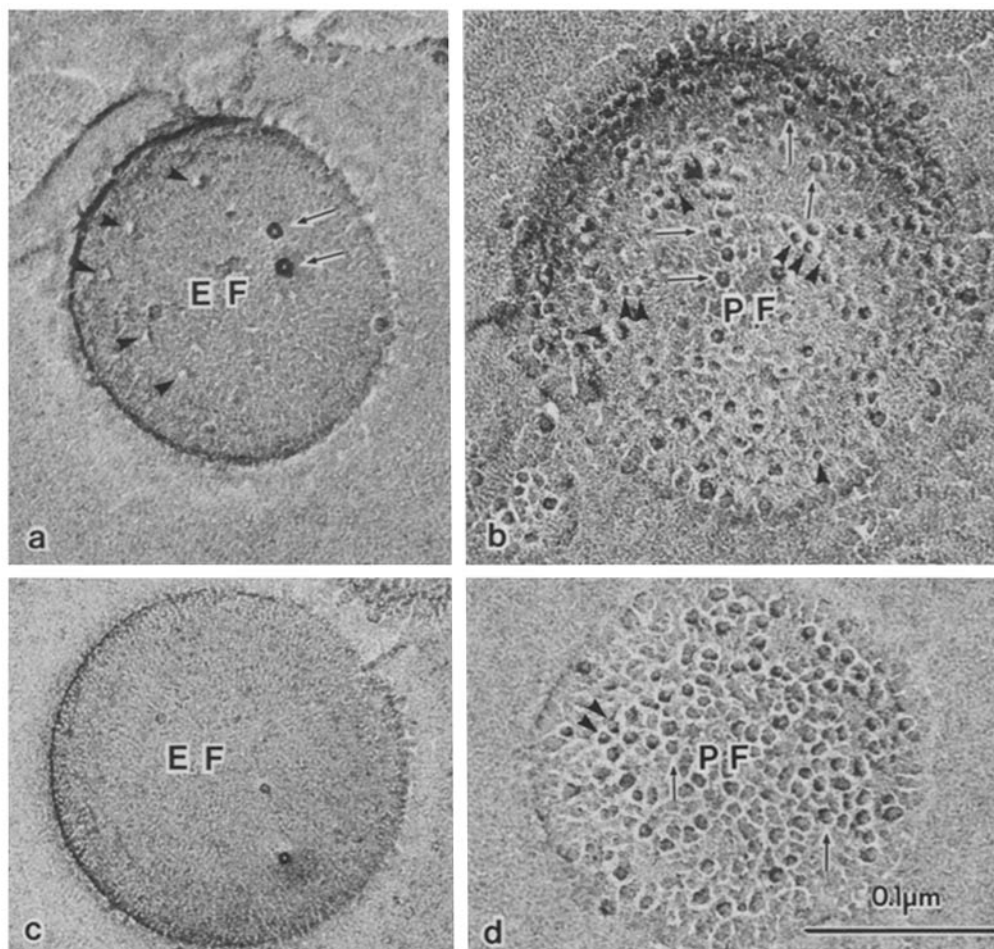


FIGURE 6 Freeze-fracture replica comparison of terminal cisternae with light SR. The E and P faces of the terminal cisternae (a and b) are compared with light SR (longitudinal cisternae) (c and d). The replicas were prepared by rotary shadowing. In a regularly spaced pits, 4–5 nm in diameter, can be observed on the E face (arrowheads), which are not seen in light SR. Occasionally large cylindrical particles with hollow centers can also be observed (arrows). Rotary shadowing reveals two different size particles in the P face of both terminal cisternae (b) and longitudinal SR (d). Most abundant are the more usual 7–8 nm (arrows) particles referable to the  $\text{Ca}^{2+}$  pump protein (arrows); the smaller particles, ~4–6 nm (arrowheads), are less numerous.  $\times 260,000$ .

to the junctional feet is unclear. In the P face of some terminal cisternae vesicles, 4–6-nm particles are sometimes observed amidst the more typical 8-nm particles (Fig. 6b). The longitudinal cisternae also contain 4–6-nm particles which are visible only by rotary shadowing (Fig. 6d), but they are devoid of a and b above.

#### Intravesicular Contents

Electron-opaque material which stains heavily after tannic acid enhancement is observed within the lumen of the terminal cisternae vesicles (Fig. 7). Such material is not observed in the longitudinal cisternae (Fig. 4e) and corresponds largely to  $\text{Ca}^{2+}$ -binding protein (calsequestrin) (25) (Table I). The electron-opaque material sometimes has the form of ropelike filaments or strands and is attached at the luminal side of the junctional face membrane in the vicinity of the feet (Fig. 7, a–e).

Sometimes the intravesicular contents can be observed in paracrystalline array. Such arrays can be seen both in thin section (Fig. 7e) and by negative staining (Fig. 7f). The arrays appear to be composed of filaments, 5–6 nm in diameter with a center-to-center repeat spacing of 12 nm. It is interesting that the intravesicular contents, even when highly ordered in

this fashion, are attached at the inner face where the junctional feet are located (Fig. 7e). On occasion, some sections reveal what appear to be a continuity of the feet structures to the internal contents (Figs. 7, c and e and 8d).

#### Organization of the Feet Structures at the Junctional Face

Sections tangential to the junctional face of isolated terminal cisternae vesicles reveal the two-dimensional arrangement of the feet structures at the junctional face. The feet structures extending  $\sim 12 \pm 1$  nm (500 measurements) from the membrane surface, are square-shaped  $\sim 20 \pm 1$  nm (100 measurements) on each side, and alternate with spaces in a checkerboard array as observed in thin section (Fig. 8, a–d) as well as by negative staining (Fig. 8e). A diagrammatic representation of the arrangement of the feet structures at the junctional face is given in Fig. 8, f–h.

#### DISCUSSION

This study describes the isolation of an enriched terminal cisternae preparation and provides ultrastructural characterization of this portion of the sarcoplasmic reticulum as com-

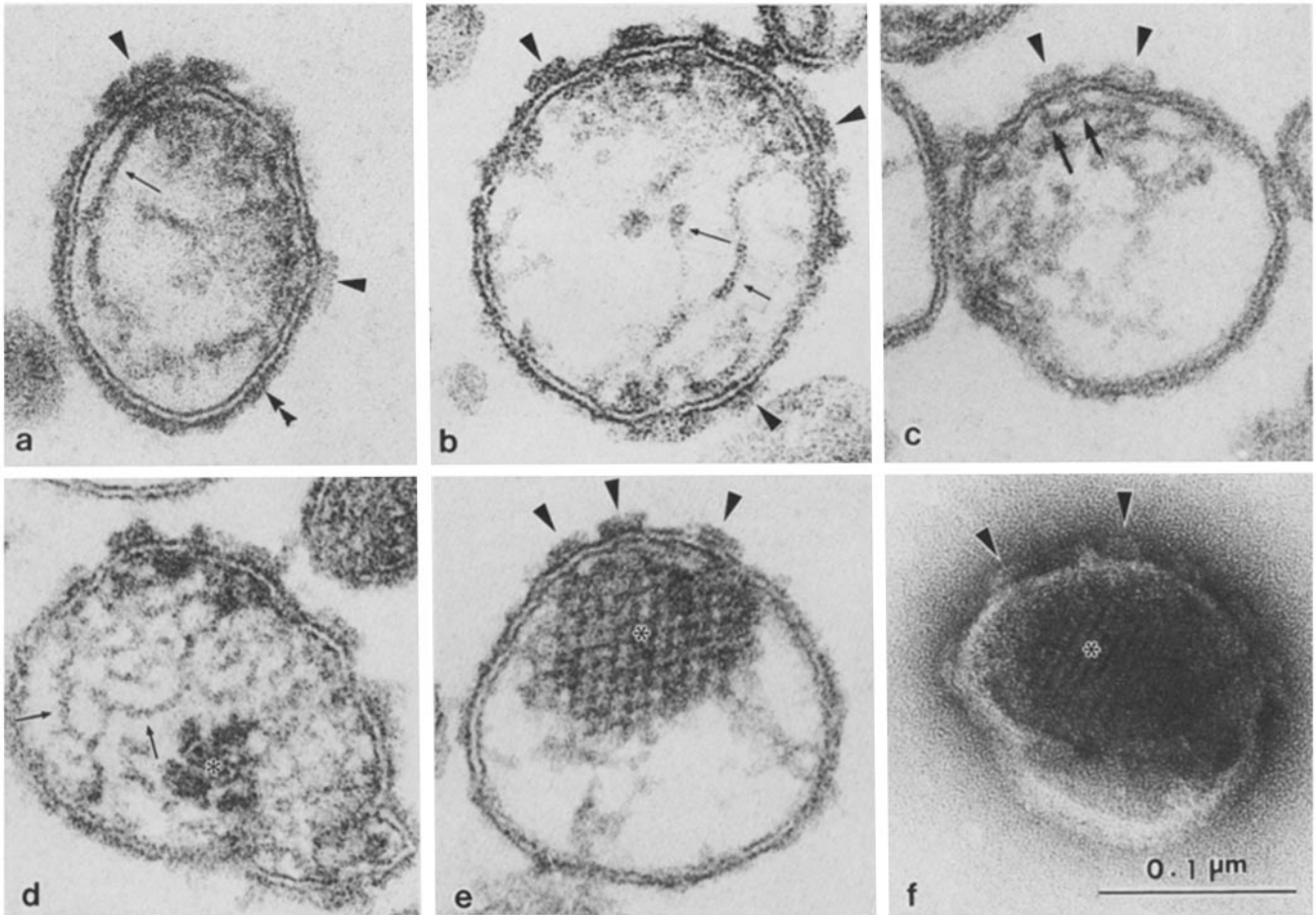


FIGURE 7 Emphasis on compartmental contents of the terminal cisternae. a–e show thin-section glutaraldehyde-OsO<sub>4</sub> fixation, a, b, d, and e were enhanced with tannic acid; f is by negative staining. The contents frequently have a ropelike appearance (a–e) or appear aggregated (d, asterisk). Occasionally, the contents appear paracrystalline (\*) in thin section (e) or by negative staining (f). × 260,000.

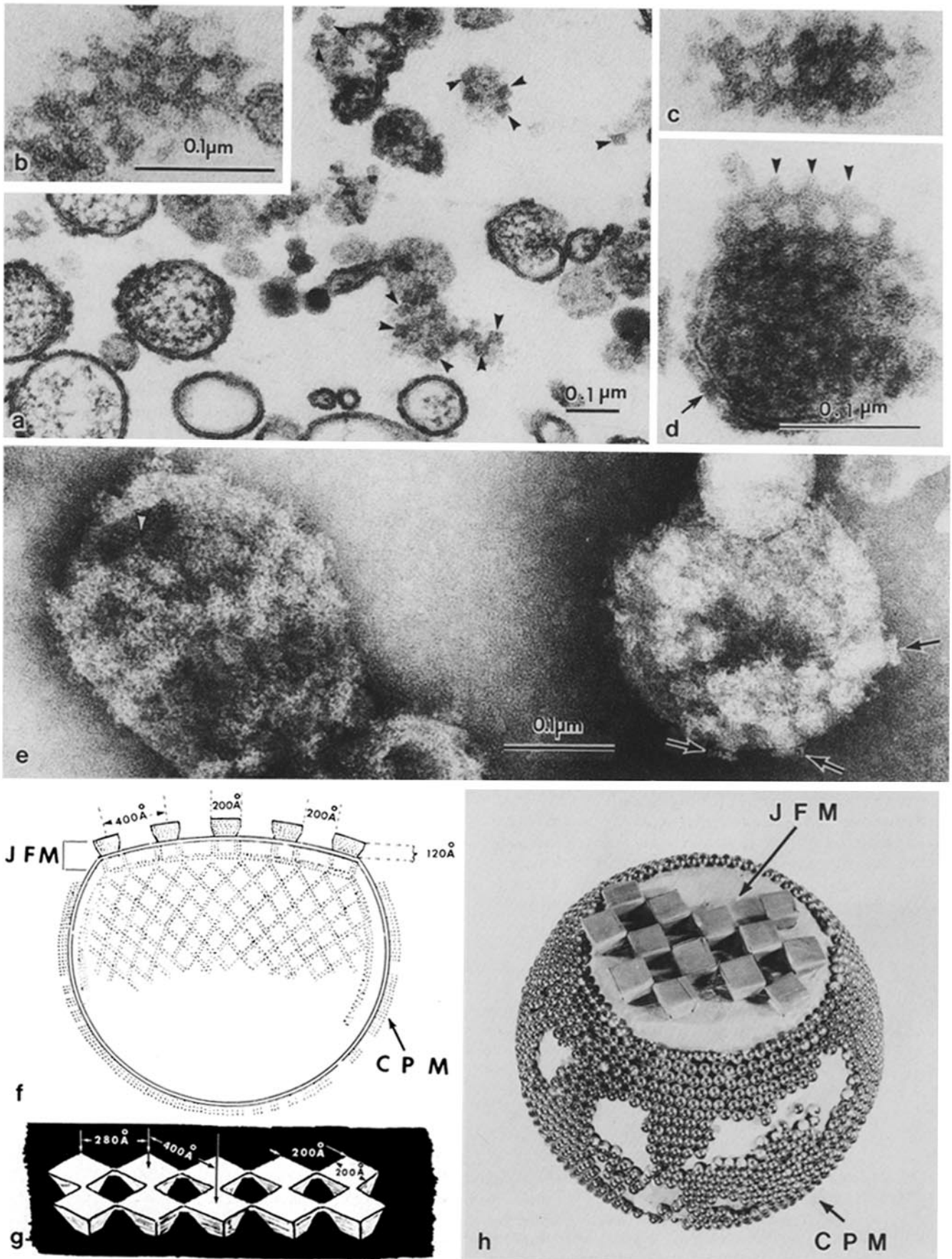
pared with longitudinal cisternae isolated from the same preparation. Terminal cisternae vesicles consist of two types of membranes, i.e., the Ca<sup>2+</sup> pump-containing membrane and the “junctional face membrane.” We have estimated that ~16% of the membrane is junctional face membrane, the remainder is Ca<sup>2+</sup> pump-containing membrane. The availability of the enriched terminal cisternae fraction enabled detailed characterization of the junctional face membrane and the junctional feet structures. The checkerboard array,

consisting of square-shaped feet structures and spaces, is clearly visualized in thin sections parallel to the junctional face (Fig. 8). Essentially complementary structural information is obtained from each of the three methods of sample preparation including the observation that the junctional face membrane is devoid of Ca<sup>2+</sup> pump protein.

Examination of freeze-fracture replicas of the terminal cisternae reveals the unique ultrastructure characteristic of the junctional face membrane. Ropelike structures, in the P face,

FIGURE 8 Structure of terminal cisternae. (a) The shape and arrangement of the junctional face are revealed in thin section. × 50,000. (b–d) Numerous feet structures are observed (arrowheads) in sections approximately parallel to the junctional face. × 260,000. The arrays of alternating square-shaped feet, 20 nm on each side, and spaces give a checkerboardlike lattice (arrowheads) observed in thin section (b–d) and by negative staining (e). In d, the checkerboard array (arrowheads) appears contiguous with the compartmental contents of the vesicle. The repeat distance between arrowheads is 28 nm. The membrane containing a foot structure can be seen on the far end of the vesicle (arrow). (e) Feet structures can also be seen at the perimeter of the negatively stained vesicle (arrow). × 260,000. Diagrammatic representations of the junctional face membrane are shown in f–h. The junctional feet and intervening spaces are depicted as square-shaped, with checkerboard lattice arrangement (g and h). Two types of membranes are shown (f and h). The junctional face membrane (JFM) at the upper surface contains the feet structures. The remainder is Ca<sup>2+</sup> pump-containing membrane (CPM). In this context, the following characteristics may be noted: (i) the junctional face is distinct from the Ca<sup>2+</sup> pump-containing membrane; (ii) the junctional feet are 20 nm on each side with a center-to-center spacing of 40 nm and extend 12 nm from the surface of the junctional face; (iii) the junctional face is devoid of Ca<sup>2+</sup> pump protein; (iv) the remainder of the membrane is Ca<sup>2+</sup> pump-containing membrane; (v) the presence of the intravesicular electron-dense material, which is sometimes arranged in filamentous or even paracrystalline arrays; (vi) the intravesicular contents are attached to the junctional face membrane.





are described for the first time in regions devoid of the 7–8-nm intramembrane particles (5). These structures appear to anchor the  $\text{Ca}^{2+}$ -binding protein. By contrast, the 7–8-nm particles, referable to the  $\text{Ca}^{2+}$  pump protein (38), are observed in the  $\text{Ca}^{2+}$  pump-containing membrane of the terminal cisternae and throughout the longitudinal cisternae. Thin-section and negative-staining electron microscopy of isolated terminal cisternae confirmed that the junctional face of the terminal cisternae is devoid of  $\text{Ca}^{2+}$  pump protein. In support of these findings, indirect immunoferritin labeling of frozen sections indicated that the  $\text{Ca}^{2+}$  pump protein was localized in the longitudinal SR and in the nonjunctional regions of the terminal cisternae (18). The model of the terminal cisternae and the junctional face presented here (Fig. 8, *f* and *h*) builds upon and extends that of the SR/transverse tubule junction presented by Franzini-Armstrong and Franzini-Armstrong and Nunzini (11, 13, 14) and others (e.g., 6, 19, 20).

In this laboratory, Mitchell et al. (27) described an enriched preparation of isolated triads. Negative staining of the triads showed that the junctional feet structures sometimes appeared to be attached to each other. In this study, the feet structures on the isolated terminal cisternae also occasionally appeared to be attached to one another (Fig. 4*b*). This can now be explained by the angle of the section with respect to the checkerboard arrangement of the feet structures on the junctional face (Fig. 8).

#### Comparison With Other Heavy SR Preparations

Several groups have reported isolation of heavy SR corresponding to terminal cisternae (3, 22, 23, 25, 28, 35, 37). In this laboratory, Meissner (25) reported the first subfractionation of highly purified SR vesicles into light and heavy SR vesicles and related them to longitudinal and terminal cisternae, respectively. This was based on the observation that the electron-opaque contents in the heavy SR matched that observed in situ in terminal cisternae, whereas longitudinal cisternae and light SR were devoid of such contents. The electron-opaque contents were shown to be referable largely to the  $\text{Ca}^{2+}$ -binding protein (calsequestrin) (9, 25). However, the heavy SR, prepared according to Meissner (25), which contained electron-opaque intraluminal contents, was isolated using salt extraction and did not show characteristic junctional feet structures. The preparation averaged smaller vesicles than those reported here and was more uniformly stained with tannic acid in the outer trilayer of the membrane (data not shown). The heavy SR which is not salt-extracted resembles the preparation we now obtain by subfractionation of microsomes obtained from the first supernatant (i.e., fraction 4 obtained from the first homogenization of muscle) in that it contains some junctional feet but fewer than the terminal cisternae fraction. This fraction appears to be similar to the heavy SR vesicles reported by Campbell et al. (3), which is essentially a modification of the light and heavy SR preparation by Meissner (25) in which no salt extraction was used. We analyzed the preparation described by Campbell et al. (3) and found that 11% of the sections contained feet structures and, of these vesicles, 23% of the perimeter was junctional face membrane; the percentage of surface area occupied by the feet was found to be 2.5%. The lower content of junctional feet, in this fraction which was not salt-extracted suggests that (*a*) heavy SR may be derived from a different portion of the terminal cisternae, which may be nonjunctional in origin, and/or (*b*) the feet structures may have been lost in the

isolation procedure.

The electron-opaque contents consist mainly of  $\text{Ca}^{2+}$ -binding protein (9, 22, 25). The latter has been purified and its properties characterized. There is evidence that the  $\text{Ca}^{2+}$ -binding protein changes conformation and aggregates in the presence of  $\text{Ca}^{2+}$  (15, 29). It has been suggested that high salt concentrations cause  $\text{Ca}^{2+}$  to be released and may result in less aggregated intraluminal contents (3). This is consistent with earlier studies showing that the binding of  $\text{Ca}^{2+}$  to purified  $\text{Ca}^{2+}$ -binding protein is practically eliminated in the presence of isotonic salt (26).

The anchoring of the electron-opaque contents in our terminal cisternae preparation is in the vicinity of the feet structures. Brunschwig et al. (1) previously noted that the electron-opaque contents were anchored on the intraluminal side of the membrane across from the feet structures and from "thickenings" on the extravascular face. Such thickenings may be referable to disfigured feet. We observe the intraluminal contents to be paracrystalline (Fig. 7, *e* and *f*) and ropelike (Fig. 7, *a-d*) and to appear to be anchored to the junctional face membrane by ropelike fibers (Figs. 5, *e-g*). When the terminal cisternae vesicles were treated with high ionic strength (0.6 M KCl) solutions, the intraluminal proteins were no longer paracrystalline or aggregated but were more uniformly dispersed (data not shown). The  $\text{Ca}^{2+}$ -binding protein has been shown by analysis of isolated heavy SR (25) or terminal cisternae (this study), and by immunocytochemistry (17) to be restricted to the terminal cisternae region of the SR. The anchoring of the  $\text{Ca}^{2+}$  binding protein near the junctional face may explain its localization in this portion of the SR.

#### Comparison with In Situ Studies

The membranes within muscle have been extensively studied in situ (7, 10, 11, 13, 14, 19, 20, 31). The availability of isolated terminal cisternae makes possible a detailed study of morphology which cannot be readily observed in situ. Negative staining can be applied to the isolated preparation to reveal surface structure (see especially Fig. 8*e*). Stain penetration is also better controlled in isolated preparations. The high enrichment of a particular type of membrane preparation, in vitro, increases the probability of making important observations such as the two-dimensional organization of the feet structures at the junctional face (Fig. 8). The important features of the terminal cisternae can then be related back to the in situ structure (Figs. 4*f* and 8). The availability of an enriched fraction also permits parallel biochemical and morphological characterization.

In summary, the terminal and longitudinal cisternae fractions described here have enabled us to carry out a detailed characterization of the morphology of the SR that correlates with in situ morphology. The terminal cisternae consist of two distinct types of membranes, the junctional face membrane and the  $\text{Ca}^{2+}$  pump-containing membrane. Longitudinal cisternae of SR consist only of the second type of membrane. Electron-opaque contents, referable largely to the  $\text{Ca}^{2+}$ -binding protein, are present only in the terminal cisternae and appear to be anchored by ropelike filaments in the junctional face membrane.

The authors acknowledge helpful discussions with Dr. Robert Mitchell, Dr. Philip Palade, Dr. Pompeo Volpe, Dr. Andreas Maurer, and Dr. Brian Costello. We thank Christine Dettbarn, Mark Dixon, and

Eunice Ogunbunmi for assisting in the biochemical analyses and Kristina Roth for typing the manuscript.

These studies were supported in part by grants from the National Institutes of Health AM 14632 and the Muscular Dystrophy Association. Dr. Alice Chu is a postdoctoral fellow of the National Institutes of Health (AM 07016).

Received for publication 13 March 1984, and in revised form 29 May 1984.

## REFERENCES

1. Brunschwigg, J. P., N. Brandt, A. H. Caswell, and D. S. Lukeman. 1982. Ultrastructural observations of isolated intact and fragmented junctions of skeletal muscle by use of tannic acid mordanting. *J. Cell Biol.* 93:533-542.
2. Cadwell, J. J. S., and A. H. Caswell. 1982. Identification of a constituent of the junctional feet linking terminal cisternae to transverse tubules in skeletal muscle. *J. Cell Biol.* 93:543-550.
3. Campbell, K. P., C. Franzini-Armstrong, and A. E. Shamo. 1980. Further characterization of light and heavy sarcoplasmic reticulum vesicles. Identification of the "sarcoplasmic reticulum feet" associated with heavy sarcoplasmic reticulum vesicles. *Biochim. Biophys. Acta.* 602:97-116.
4. Caswell, A. H., Y. H. Lau, and J. P. Brunschwigg. 1976. Ouabain-binding vesicles from skeletal muscle. *Arch. Biochem. Biophys.* 176:417-430.
5. Deamer, D. W., and R. J. Baskin. 1969. Ultrastructure of sarcoplasmic reticulum preparations. *J. Cell Biol.* 42:296-307.
6. Eisenberg, B. R., and R. S. Eisenberg. 1982. The T-SR junction in contracting single skeletal muscle fibers. *J. Gen. Physiol.* 79:1-19.
7. Eisenberg, B. R., and A. Gilai. 1979. Structural changes in single muscle fibers after stimulation at a low frequency. *J. Gen. Physiol.* 74:1-16.
8. Fleischer, S., B. Fleischer, and W. Stoerkenius. 1967. Fine structure of lipid-depleted mitochondria. *J. Cell Biol.* 32:193-208.
9. Fleischer, S., C. T. Y. Wang, A. Saito, M. Pilarska, and J. O. McIntyre. 1979. Structural studies of sarcoplasmic reticulum *in vitro* and *in situ*. In *Cation Flux across Biomembranes*. Y. Mukohata and L. Packer, editors. Academic Press, Inc., New York, 193-205.
10. Franzini-Armstrong, C. 1970. Studies of the triad. I. Structure of the junction in frog twitch fibers. *J. Cell Biol.* 47:488-499.
11. Franzini-Armstrong, C. 1975. Membrane particles and transmission at the triad. *Fed. Proc.* 34:1382-1389.
12. Franzini-Armstrong, C. 1977. The comparative structure of intracellular junctions in striated muscle fibers. In *Pathogenesis of Human Muscular Dystrophies*. L. Rowland, editor. Excerpta Medica, Amsterdam, 612-625.
13. Franzini-Armstrong, C. 1980. Structure of sarcoplasmic reticulum. *Fed. Proc.* 39:2403-2409.
14. Franzini-Armstrong, C., and C. Nunzi. 1983. Junctional feet and particles in the triads of a fast-twitch muscle fiber. *J. Muscle Res. Cell Motil.* 4:233-252.
15. Ikemoto, N., B. Nagy, G. M. Bhatnager, and J. Gergely. 1974. Studies on a Metal-binding protein of the sarcoplasmic reticulum. *J. Biol. Chem.* 249:2357-2365.
16. Ikemoto, N., F. A. Sreter, A. Nakamura, and J. Gergely. 1968. Tryptic digestion and localization of calcium uptake and ATPase activity in fragments of sarcoplasmic reticulum. *J. Ultrastruct. Res.* 23:216-232.
17. Jorgensen, A. O., V. L. Kalnins, and D. H. MacLennan. 1979. Localization of sarcoplasmic reticulum proteins in rat skeletal muscle by immunofluorescence. *J. Cell Biol.* 80:372-384.
18. Jorgensen, A. O., A. C. Y. Shen, D. H. MacLennan, and K. T. Tokugasu. 1982. Ultrastructural localization of the  $Ca^{2+}$  +  $Mg^{2+}$ -dependent ATPase of sarcoplasmic reticulum in rat skeletal muscle by immunoferritin labeling of ultrathin frozen sections. *J. Cell Biol.* 92:409-416.
19. Kelly, D. E. 1969. The fine structure of skeletal muscle triad junctions. *J. Ultrastruct. Res.* 29:37-49.
20. Kelly, D. E., and A. M. Kuda. 1979. Subunits of the triadic junction in fast skeletal muscle as revealed by freeze-fracture. *J. Ultrastruct. Res.* 68:220-233.
21. Laemmli, U. K. 1970. Cleavage of structural proteins during the assembly of the head of bacteriophage T4. *Nature (Lond.)* 227:680-685.
22. Lau, Y. H., A. H. Caswell, and J. P. Brunschwigg. 1977. Isolation of transverse tubules by fractionation of triad junctions of skeletal muscle. *J. Biol. Chem.* 252:5565-5574.
23. Louis, C. F., P. A. Nash-Adler, G. Fudyma, M. Shigekowa, A. Akowitz, and A. M. Katz. 1980. A comparison of vesicles derived from terminal cisternae and longitudinal tubules of sarcoplasmic reticulum isolated from rabbit skeletal muscle. *Eur. J. Biochem.* 111:1-9.
24. Lowry, O. H., N. J. Rosenbrough, A. L. Farr, and R. J. Randall. 1951. Protein measurement with the Folin phenol reagent. *J. Biol. Chem.* 193:265-275.
25. Meissner, G. 1975. Isolation and characterization of two types of sarcoplasmic reticulum vesicles. *Biochim. Biophys. Acta.* 389:51-68.
26. Meissner, G., G. Conner, and S. Fleischer. 1973. Isolation of sarcoplasmic reticulum by zonal centrifugation and purification of  $Ca^{2+}$ -Pump and  $Ca^{2+}$ -binding proteins. *Biochim. Biophys. Acta.* 298:246-269.
27. Mitchell, R. D., A. Saito, P. Palade, and S. Fleischer. 1983. Morphology of isolated triads. *J. Cell Biol.* 96:1017-1029.
28. Miyamoto, H., and E. Racker. 1981. Calcium-induced calcium release at terminal cisternae of skeletal sarcoplasmic reticulum. *FEBS (Fed. Eur. Biochem. Soc.) Lett.* 133:235-238.
29. Ostwald, T. J., D. H. MacLennan, and K. J. Dorrington. 1974. Effects of cation binding on the conformation of calsequestrin and the high affinity calcium-binding protein of sarcoplasmic reticulum. *J. Biol. Chem.* 249:5867-5871.
30. Palade, P., A. Saito, R. D. Mitchell, and S. Fleischer. 1983. Preparation of representative samples of subcellular fractions for electron microscopy by filtration with dextran. *J. Histochem. Cytochem.* 31:971-974.
31. Peachey, L. D. 1965. The sarcoplasmic reticulum and transverse tubules of the frog's sartorius. *J. Cell Biol.* 25:209-231.
32. Rouser, G., and S. Fleischer. 1967. Isolation, characterization and determination of polar lipids in mitochondria. *Methods Enzymol.* 10:385-406.
33. Saito, A., S. Seiler, and S. Fleischer. 1984. Alterations in the morphology of rabbit skeletal muscle plasma membrane during membrane isolation. *J. Ultrastruct. Res.* In press.
34. Saito, A., C.-T. Wang, and S. Fleischer. 1978. Membrane asymmetry and enhanced ultrastructural detail of sarcoplasmic reticulum revealed with use of tannic acid. *J. Cell Biol.* 79:601-606.
35. Salvati, G., P. Volpe, S. Salvatore, R. Betto, E. Damiani, A. Margreth, and I. Pasquale-Ronchetti. 1982. Biochemical heterogeneity of skeletal-muscle microsomal membrane. *Biochem. J.* 202:289-301.
36. Somlyo, A. V. 1979. Bridging structures spanning the junctional gap at the triad of skeletal muscle. *J. Cell Biol.* 80:743-750.
37. Van Winkle, W. B., R. J. Bick, D. E. Tucker, C. A. Tate, and M. L. Entman. 1982. Evidence for membrane microheterogeneity in the sarcoplasmic reticulum of fast twitch skeletal muscle. *J. Biol. Chem.* 257:11689-11695.
38. Wang, C.-T., A. Saito, and S. Fleischer. 1979. Correlation of ultrastructure of reconstituted sarcoplasmic reticulum membrane vesicles with variation in phospholipid-to-protein ratio. *J. Biol. Chem.* 254:9209-9219.
39. Warren, G. B., P. A. Toon, N. J. M. Birdsall, A. G. Lee, and J. C. Metcalfe. 1974. Reconstitution of a calcium pump using defined membrane components. *Proc. Natl. Acad. Sci. USA.* 71:622-626.